RSC Advances

One-step biofabrication of copper nanoparticles from Aegle marmelos Correa aqueous leaf extract and evaluation of its anti-inflammatory and mosquito larvicidal efficacy

Journal:	*RSC Advances*
Manuscript ID:	RA-ART-09-2014-010003.R1
Article Type:	Paper
Date Submitted by the Author:	25-Sep-2014
Complete List of Authors:	Angajala, Gangadhara; VIT University, Chemistry pasupala, Pavan; VIT University, Chemistry Subashini, Radhakrishnan; VIT University, Organic Chemistry Division

One-step cost effective biofabrication of copper nanoparticles from *Aegle marmelos* correa aqueous leaf extract and evaluation of its anti-inflammatory and mosquito larvicidal efficacy

Gangadhara Angajala, Pasupala Pavan, R. Subashini*

Chemistry Research Laboratory, Organic Chemistry Division. School of Advanced Sciences, VIT University, Vellore - 632014.

*Corresponding author:
Tel.: +91 94435 41305, +91 0416 2202352.
Email address: dr.subashini.r@gmail.com (Dr. R. Subashini)

Graphical abstract

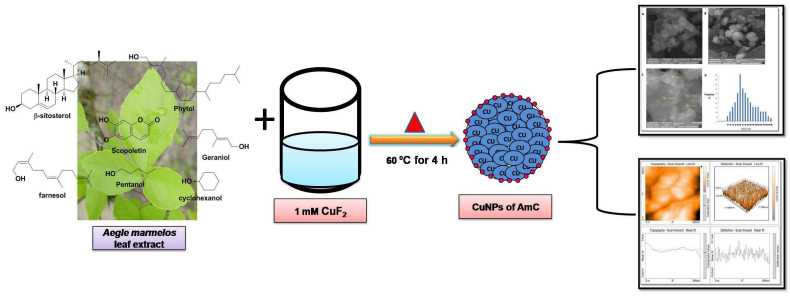

Highlights

Biofabrication of CuNps from AmC aqueous leaf extract of various sizes with good anti-inflammatory and mosquito larvicidal efficacy.

Cite this: DOI: 10.1039/c0xx00000x

www.rsc.org/xxxxxx

ARTICLE TYPE

One-step biofabrication of copper nanoparticles from *Aegle marmelos* Correa aqueous leaf extract and evaluation of its anti-inflammatory and mosquito larvicidal efficacy.

Gangadhara Angajala, Pasupala Pavan, R. Subashini*

Received (in XXX, XXX) Xth XXXXXXXXX 20XX, Accepted Xth XXXXXXXXX 20XX
DOI: 10.1039/b000000x

The present investigation is focused on biofabrication of copper nanoparticles (CuNPs) by using *Aegle marmelos* Correa aqueous leaf extract as a reducing agent. The synthesized CuNPs were sucessfully characterized by UV-Vis spectroscopy, FT-IR, XRD, SEM and AFM studies. Phytosynthesis of CuNPs was done at room temperature (30 ºC) for 24 h and at 60 ºC, 100 ºC for 4 h. The green synthesis of spherical shaped CuNPs biofabricated from *Aegle marmelos* Correa having face centered cubic structure showing an average particle size of 50-100 nm, 100-200 nm which is in consistent with the particle size calculated by XRD Scherer equation were reported. We further explored *in-vitro* anti-inflammatory and mosquito larvicidal efficacy of biosynthesized CuNPs with crude leaf extracts of *Aegle marmelos* Correa against three blood feeding parasites namely *Anopheles stephensi, Aedes aegypti* and *Culex quinquefasciatus*. A comparative study has been done on the bioefficacy of different sizes of CuNPs coated with *Aegle marmelos* Correa with that of CuNPs synthesized by chemical reduction method using $NaBH_4$. The results obtained clearly shows that CuNPs (50-100 nm) of *Aegle marmelos* Correa possess good anti-inflammatory efficacy showing percentage inhibition of 78.90 ±1.23 for membrane stabilization method and 74.18 ± 1.48 for albumin denaturation method at a concentration of 100 µg/ml which is comparable to standard Aceclofenac and better larvicidal activity against *Anopheles stephensi* with an LC_{50} of 500.06 ppm when compared to crude leaf extracts of *Aegle marmelos* Correa and that of standard Temephos.

1 Introduction

Over the last few years the development of green processes for the production of nanomaterials have gained much attention by simultaneously evolving into a significant branch of nanotechnology and evenly poised throughout the world [1,2]. Nanoscale materials possess good therapeutic effects owing to its high surface area to volume ratio. Nanoparticles demonstrate unique properties with potentially wide range of applications and thereby provides useful platform to explore various interdisciplinary areas, as a result nanoparticles have high demand due to their wide spread applicability in various fields [3-5]. One of the core values of medicine is an early and accurate diagnosis of clinical parameters, providing an effective treatment without side effects. So with the tremendous growth in nanotechnology and nanomedicine the achievement of these goals is made quite easier than ever.

Now a day there is a growing need to develop reliable ecofriendly process for the synthesis of nanoparticles and hence the major focus has been turned towards green chemistry [6, 7]. Biogenic synthesis of nanomaterials using plant extracts is still considered as a favourite method for green production of nanomaterials mainly because of its simplicity, ecofriendliness and economically viable nature compared to the chemical methods. The active functional organic groups present in the plant extract play a key role in the synthesis of nanoparticle by acting as reducing, stabilizing and capping agents [8-14]. Nanomaterials designed by means of plants present good polydispersity, dimensions and stability. The biological effectiveness of nanoparticles is directly proportional to their specific surface area due to increase in surface energy. Copper is well known to play a major role in biological activities such as antioxidant, regeneration of damaged tissue, and incorporation of Fe into Hb, nerve conduction, cardiovascular system, estrogen metabolism and immune system. Copper also play a key role in the synthesis of antioxidant called copper superoxide dismutase (SOD). It is also considered as important stimulant for monoamine oxidase and neurotransmitters like epinephrine, nor epinephrenine and dopamine. Copper is the third most abundant mineral present in the body especially found in brain and liver which possess wide range of biological applications such as anti-inflammatory, antiarthritic, antiepileptic, wound healing and tissue remodeling [15-25].

Aegle marmelos Correa commonly called bael tree belongs to the family Rutacae, monotypic genera of sub family Aurantioideae. It originates from India and usually grows in outer Himalayan and south Indian plateau regions with an altitude ranging from 200-1300 m. The tree is considered as herbal medicine for the treatment of various ailments infact, each and every part of its plant has its own medicinal property [26-31]. Most of the secondary metabolites of *Aegle marmelos* Correa contain -OH as functional group in their chemical structure which has the ability to reduce metal salts into nanoparticles. The role of -OH group in various plants as reducing, stabilizing and capping agents during the biosynthesis of metal nanoparticles was previously reported [32].

In the present research we are reporting the phytofabrication of CuNPs using aqueous leaf extracts of AmC. In continuation to this we also explored and compared *in-vitro* anti-inflammatory and mosquito larvicidal efficacy for CuNPs of AmC with that of crude aqueous, methanol and ethyl acetate leaf extracts.

2 Results and discussion

2.1 GC-MS analysis of AmC leaf extract

The chemical constituents of leaf extract of AmC were analyzed by using Perkin Elmer GC-MS (clarus 680/600) having 5973 N mass selective detector equipped with split or split less capillary injection port (30.0 m × 240 µm). An intial oven temperature of 60 ºC was programmed for 2 min, later a steady rise in temperature of 10 ºC/ min was maintained upto 300 ºC. The inlet and mass transfer temperatures were set as 250 ºC and 280 ºC respectively. Helium gas was used as a carrier gas at constant flow of 1.0 ml/min and sample was injected with a split ratio of 10:1. An electron ionization system with ionization energy of 70eV was used. The composition of AmC leaf extract was identified after comparing with the library. (Table 1) shows the constituents of leaf extracts of AmC, percentage composition, molecular weight and retention time which were listed in their order of elution. A total of 17 compounds were identified from GC-MS analysis representing 92.83% of total composition of leaf extract. The major compounds identified by comparing with the library include β-sitosterol (55.65 %), camphene (5.67 %), α-phellandrene (4.79 %) and phenylethylcinnamide (4.02 %). The percentage composition of the remaining compounds ranged from 0.31 % to 3.75 % (Fig. 1).

2.2 UV-Visible spectrum of copper nanoparticles

The UV-Visible spectrum of CuNPs of AmC in water was recorded against time of reaction by using UV-Visible spectrophotometer. The formation of CuNPs of AmC was monitored in the range of 200-500 nm where distinct broad band observed at 270 and 274 nm in the ultraviolet region which was very close to the calculated optical spectrum of various metal nanoparticles both in water and in vacuum by Creighton and Eadon based on Mie's theory [33]. The intensity of the peak could be attributed to the concentration of the reducing agents present in aqueous leaf extract of AmC. The exact position of surface plasmon mainly depends on particle size and stability of the corresponding CuNPs [34]. The broad peaks at 270 and 274 nm is due to interband transition of copper electron from deep level of valence band. The blue shift in the peak centered at 270 nm (for 100 ˚C) when compared to 274 nm (for 60 ˚C) in the absorption spectra was mainly due to increase in temperature which causes transition of electrons from the more inner shell of the copper to the upper most shell. Due to aggregation and agglomeration the size of the nanoparticle substantially increases as a result the material settled down at the bottom of the container causing a decrease in the absorption. The colour of the solution gradually changed from dark green to light yellow indicating the generation of CuNPs from aqueous leaf extracts of AmC. (Fig.2A & 2B).

2.3 Fourier transformed infrared (FTIR) spectroscopy

The FT-IR analysis showed the characteristics of formation of CuNPs of AmC. The broad absorption band centered at 3446.79 and 3437.15 cm^{-1} corresponds to the O-H stretching vibrations of CuNPs of AmC and aqueous leaf extract of Amc showing 9 units red shift of this polar group. This is mainly due to the interaction of CuNPs with -OH group of the corresponding aqueous leaf extracts which indicates that AmC assist in coordinate with Cu^{2+} ions [35]. The broadness of the band indicates that the nanoparticles are in crystalline nature. The weak band near 1631.78 cm^{-1} was assigned to C=O which is probably due to the interaction of various bioactive compounds of aqueous leaf extract of AmC with metal surface of the copper producing charge delocalization in double bond and thereby behaves as pseudo double bond between carbon and oxygen. These observations provided the evidence for the presence of hydroxyl group which act as reducing as well as stabilizing agents during the formation of CuNPs. The absorption band at 2935.66 cm^{-1} in aqueous leaf extract of AmC corresponds to C=C stretching vibrations of β-sitosterol of AmC which is observed to shift to lower wave number in CuNPs of AmC (2927.94 cm^{-1}) and the decrease in intensity of the band gives an idea that β-sitosterol of AmC involved in the reduction of Cu^{2+} ions to CuNPs. The absorption bands serrated in the region 1000-1500 cm^{-1} are assigned to C-O stretching vibrations and O-C=O symmetric and asymmetric stretching vibrations of organic phases surrounding the CuNPs. The band around 931.62 cm^{-1} corresponds to C=O stretching vibrations (Fig.3A & 3B).

2.4 X-ray diffraction pattern of copper nanoparticles

XRD analysis of CuNPs of AmC showed three intense peaks in the spectrum 2θ scale ranging from 10 to 80. The XRD pattern of synthesized CuNPs of AmC agree well with the standard pure crystalline copper structures published by the Joint Committee on Powder Diffraction standards (File no: 04-0836) confirmed that biosynthesized CuNPs are in crystalline form with face centered cubic (FCC) structure. The presence of CuNPs of AmC at 60 ˚C results in the formation of Bragg's peaks at 2θ values of 44.93º, 50.78º and 75.02º can be indexed as (111), (220), (200) planes of FCC copper (Fig.3C). The unidentified peaks (*) at 2θ values of 17.08º, 24.64º and 32.63º corresponds to crystalline and amorphous organic phases of aqueous leaf extract of AmC respectively accompanying the CuNPs. Similarly the presence of CuNPs of AmC at 100 ˚C results in the formation of Bragg's peaks at 2θ values of 44.27º, 50.36º and 74.08º can be indexed as (111), (220), (200) planes of FCC copper (Fig.3D). The mean diameter of nanoparticles was calculated from the XRD pattern by using Sherrer formula, $d = 0.94 \lambda/\beta \cos\theta$ where'd' is the mean diameter of the nanoparticles, λ is wavelength of X-ray radiation source, β is the angular FWHM (full width at half-maximum) of the XRD peak at the diffraction angle θ. The mean diameter was determined to be 60 ± 5 nm for CuNPs of AmC at 60 ˚C and 110 ± 5 nm for CuNPs of AmC at 100 ˚C.

2.5 Scanning electron microscopy

The surface morphology of the synthesized CuNPs of AmC was studied by using SEM. The results obtained from SEM showed spherical shaped nanoparticles having an average particle size of 50-100 nm for CuNPs at 60 ˚C (Fig.4A & 4B) and 100-200 nm for CuNPs at 100 ˚C (Fig.4D & 4E) which reveals that all CuNPs of AmC are agglomerated forming polydisperse nanoparticles showing irregular shapes with narrow particle size distribution. At high temperature (100 ˚C) due to instantaneous multiple nucleations and vigorous particle movements resulted in more agglomeration of the corresponding nanoparticles. This high rate of agglumeration favours growth of nanoparticles and therefore the concentration of the copper atoms begins to decrease sooner,

leading to the generation of fewer numbers of nanoclusters and hence there is significant increase in size of the CuNPs. The size distribution of the CuNPs was calculated by using (Shodor-Interactivate © 1994-2014 software; version 3.0). The average particle size calculated with XRD is in consistent with the SEM results. (Fig.4C-4F). The SEM images gives a clear idea that CuNPs are surrounded by a layer of organic biomaterial derived from AmC leaf extract having surface functional -OH groups which actively participate in reduction of copper to copper nanoparticles in addition they also act as capping and stabilizing agents (Fig.5A & 5B).

2.6 Atomic force microscopy

AFM is an advance method for characterizing the CuNPs of AmC. For this study the supernatant of the solution was taken in eppendroff tube and kept in sonicator for 15 minutes at room temperature. After this 1 drop of the sample placed on thin glass slide and dried well by flushing nitrogen. AFM images were taken with silicon cantilever having force constant of 0.02-0.77 N/m, tip height 10-15 nm, contact mode. The results obtained from AFM showed that the biomaterial surrounding the CuNPs was agglomerated forming distinct nanostructures. The surface area of irregular CuNPs and nano island formation is evident apart from dense copper nanoclusters. Further the surface area of CuNPs increased dramatically during stabilization process by various organic functional groups present in AmC. The topographical image of CuNPs of AmC (50-100 nm, 100-200 nm) was reported in (Fig.6A & 6B) which clearly shows irregular spherical shape CuNPs surrounded by rough organic agglumerates.

Copper is a trace element belongs to d-block elements in the periodic table. It is one of the most important elements discovered during ancient times and since then people started using it for many curative properties. Instead of deriving many pharmaceutically active compounds from plants most of the ancients largely relied on copper for its effectiveness in the treatment of wounds and skin disorders [36, 37]. Researchers carrying out more work to explore the efficacy of copper for the treatment of various internal diseases including cancer, rheumatoid arthritis, anemia and heart disease. The first modern research on the therapeutic efficacy of copper containing substances carried out by Professor John R. J. Sorrenson in 1966 demonstrated that copper complexes possess good therapeutic role in the treatment of inflammatory diseases using doses that are non toxic. Since copper containing metallo complexes were started being used for treating patients with chronic arthritis and other degenerative diseases. More than 150 copper complexes have been shown to show more efficacy than their parent compounds. For example copper aspirinate proved to be more effective in the treatment of rheumatoid arthritis in addition to this it also prevents the ulceration of stomach associated with aspirin therapy. The use of copper bracelets for the treatment of arthritis have been extensively used throughout the world mainly because copper in bracelet reacts with fatty acids in the skin to form copper salts that are easily absorbed in to the body. In pregnancy the demand for copper is more as it plays a critical role in normal neurological development of fetus as small deficit in copper produces substancial changes in fetal brain enzymes [38].

From the GC-MS analysis it has been found that β-sitosterol (55.65) was major compound present in crude aqueous leaf extract of AmC. In the biofabrication of CuNPs, β-sitosterol plays a major role by acting as reducing, stabilizing and capping agent. β-sitosterol is majorly a plant sterol which inhibits cholesterol absorption in the lower intestine thereby reducing excess level of cholesterol in the blood. Atherosclerosis is a chronic inflammatory disease associated with increased oxidative stress, adhesion of vascular endothelium and subsequent migration into the cells. The over expression of adhesion molecules by endothelial cells which was further activated by inflammatory cytokines leads to oxidative modification of low density lipoprotein (LDL), endothelium dysfunction and artherosclerotic leisions. Research studies proved that β- sitosterol has been associated with cardiovascular protection in artherosclerosis by mainly exerting its antioxidant defensive system in addition to this it also inhibits the over expression of vascular adhesion molecule 1, intracellular adhesion molecule 1 (VCAM-1 and ICAM-1) and the subsequent attachment of monocytes in human aortic endothelial cells (HAECs) [39]. β-sitosterol also exerts its impact on tumor necrosis factor-α (TNF- α) relating signal in HAEC such as phosphorylation and activation of nuclear factor-κB (NFκB).

The synergistic efficacy of both β-sitosterol and copper induces an enhanced antiinflammatory efficacy (Fig.7). This effect was mainly due to increase in surface area to volume ratio which automatically increases the dominance behaviour of atoms on the surface rather than the interior of the particle. This leads to an increase in the surface energy which is directly proportional to its biological effectiveness. Increase in surface area of CuNPs makes maximum interaction of β-sitosterol with the receptor site by producing its therapeutic effect. CuNPs of AmC generally decreases the systemic inflammation and simultaneously supports proliferation of pheripheral blood lymphocytes thereby enhancing the cytotoxic efficacy of natural killer cells. On the other hand CuNPs of AmC binds with GHK (glycyl-L-histidyl-L-lysine) tripeptide (Fig.8) and suppresses the inflammation by lowering the level of acute phase inflammatory cytokines TNF-alpha, TGF-beta [40].

CuNPs of AmC accompanied with β-sitosterol actively triggered by oxidative stress during inflammation, effectively eliminates free radical oxidants in the extra cellular region via H-atom donation (Fig.9A). It increases the expression of vascular endothelial growth factor and basic fibroblast growth factor which helps in the formation of blood vessel, stimulates synthesis of elastin and collagen in order to maintain the integrity of blood vessels [41]. As the surface area of CuNPs of AmC (50-100 nm) is higher than that of other particles predominantly it shows better anti-inflammatory activity with percentage inhibition of 78.90 ±1.23 for membrane stabilization method and 74.18 ± 1.48 for albumin denaturation method at a concentration of 100 µg/ml which was on par to that of standard Aceclofenac (88.24 ± 0.86 & 84.67 ± 0.19) (Table.2) This efficacy is mainly attributed to β-sitosterol of AmC surrounding the CuNPs. Due to small size copper possess unique properties regardless of their chemical properties they have high surface to volume ratio which automatically causes their physical properties dominated by their effect of capping agents (β-sitosterol) and surface atoms on the surface of CuNPs. Particles with high surface area possess many reactive sites than a particle with low surface area leading to good therapeutic efficacy. CuNPs of AmC shows antiinflammatory efficacy by protecting the human erythrocyte membrane against lysis induced by heat. Injury caused to human erythrocyte membrane will render the cell more susceptible to secondary damage through free radical induced lipid peroxidation. During the process of inflammation CuNPs of AmC effectively inhibits the release of lysosomal enzymes and stabilizes the lysosomal membrane thereby prevents the leakage of serum proteins and

fluids in to the tissues. In addition to this it also reduces oxidative damage by quenching toxic products of fattyacid lipid peroxidation and modulates iron levels thereby preventing further tissue damage (Fig.9B).

The results obtained from larvicidal efficacy gives clearly an idea that CuNps of AmC (50-100 nm) possess better larvicidal efficacy with an LC_{50} of 538.25, 508.31 and 582.73 against *Aedes aegypti, Anopheles stephensi and Culex quinquefasciatus* (Table 3, Fig. 9C) which were on par with that of standard Temephos. Sterols play an important role in the life cycle of most of the insects and mosquitoes. But unfortunately mosquitoes do not possess the ability to synthesize the sterols. During larval stage mosquitoes take sterols from the plant decays in the form of phytosterol which is further converted to cholesterol for the construction of cell membranes, development and growth. The whole process of conversion takes place with the aid of sterol carrier protein-2 (SCP-2). The SCP-2 also involved in the steroid biosynthesis by transferring cholesterol to the mitochondria. In this process inhibition of SCP-2 is considered as good therapeutic target for controlling mosquitoes in larval stage. The CuNPs of AmC inhibits SCP-2 thereby prevents the formation of cholesterol which causes mortality in mosquito larvae (Fig. 9D). CuNps of AmC at nanoscale have the advantage to penetrate easily deep inside the cell wall and acts as a competitive inhibitor for SCP-2 protein preventing their growth and development. In addition to this, it also disturbs permeability of cell membrane effectively and inhibits cellular respiration. Due to inhibition of SCP-2 mosquitoes cannot synthesize cholesterol from plant sterols which results in developmental deformities leading to larval death. The failure to discover new potent class of insecticides has led many researchers back to biodiscovery studies in search for new and economically reliable herbal insecticides. The results obtained from larvicidal efficacy showed that a small quantity of active fraction CuNPs of AmC is sufficient to inhibit the emergence of mosquito larval population.

3 Experimental

3.1 Materials and methods

3.1.1 Collection of plant material

The AmC leaves were collected from Ranipet area (12.9275 ºN, 79.3302 ºE) Vellore district, Tamil Nadu, India during the month of February 2013. The collected leaves were identified by Dr. S. Nanthakumar, Program Coordinator, Horticulture, Tamilnadu Agricultural University, Krishi Vignan Kendra, Virinjipuram-632014, Vellore district, Tamil Nadu, India. A voucher specimen has been submitted at the office for reference.

3.1.2 Preparation of leaf extract

Fresh leaves of AmC were taken and washed thoroughly with distilled water. The leaves were kept for drying in shade region for about 5 days and then finely powdered. A weighed quantity of powdered drug (20 g) was taken and extracted with 200 ml of double distilled water by using soxhlet extractor for 72 h. The extract was filtered using whatman filter paper and the filtrate was evaporated. Simultaneously a weighed quantity of powdered drug (30 g) was taken and subjected to ethylacetate followed by methanol extraction for 48 h.

3.1.3 Synthesis of copper nanoparticles

Aqueous solution (1 mM) of Copper fluoride (CuF_2) was freshly prepared with milli Q water and used for the synthesis of CuNPs of AmC. 10 ml of aqueous extract was added to 80 ml of 1 mM CuF_2 solution. The effect of temperature on the synthesis of Copper NPs was monitored both at room temperature 30 ºC for 24 h and at 60 ºC, 100 ºC on water bath for 4 h. The solid precipitate obtained after keeping at room temperature was filtered using commercially available Anodisc 13 membrane filters (pore size 0.02µm). After heating at 60 ºC, 100 ºC for 4 h the reaction was terminated and the colloidal solution was allowed to precipitate for 30 min. Later the precipitated CuNPs of AmC were centrifuged at 3500 rpm for 20 min and the solid particles settled at the bottom were separated by using Anodisc 13 membrane filters.

3.1.4 Characterization

The biogenic reduction of Cu^{2+} ion in solution was monitored by using UV–vis spectrophotometer (Jasco, model no: V-670), FT-IR spectroscopy (Shimadzu, model no: I.R affinity-1), GC-MS (Perkin Elmer: clarus 680/600). Further characterization of nanoparticles was done using XRD analysis (Advance Powder X-ray diffractometer, Bruker, Germany, model no: D8), SEM analysis (Scanning electron microscopy, Tescan Vega 3 Sbu) and AFM (Atomic Force Microscopy, Nanosurf EasyScan 2, Version 1.3).

3.2 Biological evaluation

3.2.1 *In-vitro* Anti- inflammatory Studies

In-vitro anti-inflammatory studies of synthesized CuNPs of AmC was carried out and compared with different leaf extracts of AmC by two methods such as membrane stabilization test and albumin denaturation assay as per reported method [42, 43].

A. Membrane stabilization method

Antiinflammatory agents provide membrane stabilization of RBC thereby inhibits the release of lysosomal content of neutrophil which is considered as prime cause for inflammation. Fresh human blood about 10 ml was collected from healthy volunteer and transferred to heparinized centrifugation tubes. The tubes were kept for centrifugation about 5 min at 3000 rpm. Later the tubes were washed two times with equal volumes of saline and later reconstituted as 10 v/v RBC suspensions by using normal saline.

Equal volumes of test samples of various concentrations (25, 50, 100 µg/ml) and 10 v/v RBC suspension were taken in test tubes. Normal saline solution excluding the test sample was taken and treated as control, Aceclofenac (bulk drug) was used as standard. The test tubes containing the reaction mixture were incubated on water bath at 56 ºC for 30 min. Then the solution was cooled and again kept for centrifugation about 5 min at 2500 rpm. The absorbance of supernatant liquid was taken by using UV–vis spectrophotometer at 560 nm. The experiment was carried out in triplicate.

B. Albumin denaturation assay

The ability of CuNPs of AmC to prevent heat induced protein denaturation was studied through this assay. A solution of 0.2% w/v of bovine serum albumin (BSA) was prepared in tris buffer saline and the pH was adjusted by using glacial acetic acid. A methanolic solution of test compounds of various concentrations (25, 50, 100 µg/ml) was taken in a test tube to which 5 ml BSA

was added. A control was prepared by taking 5 ml of 0.2% w/v BSA containing 50 µl of methanol and Aceclofenac (bulk drug) was used as standard. The test tubes were heated on water bath for 5 min at 72 ºC and cooled for 10 min. The absorbance of the solution was taken by using UV–vis spectrophotometer at 660 nm. The experiment was carried out in triplicate.

The percentage inhibition of membrane stabilization and albumin denaturation assay (Table 2) were calculated by:

$$\text{Percentage inhibition} = \frac{(\text{Abs}_{\text{control}} - \text{Abs}_{\text{sample}})}{\text{Abs}_{\text{control}}} \times 100$$

3.2.2 Larvicidal efficacy

Mosquito-borne diseases represent a significant threat to human life all over the world for decades. According to World Health Organization (WHO) it is estimated that nearly 1 million people die from various mosquito-borne diseases all over the world and millions of people suffered from pain and illnesses transmitted by mosquitoes [44]. The two principle approaches available to treat mosquitoes are genetic and chemical. In genetic approach research being carried out to alter genetic pathways of mosquitoes so that it cannot transmit the diseases. But releasing genetically modified organism in to the environment is still creating a lot of uncertainties in this approach. Mosquito in larval stage is considered as more significant in finding larvicidal efficacy of CuNPs of AmC due to its low mobility and modern use of persistent synthetic insecticides will results in various health and environmental hazards including biomagnification through food chain affecting aquatic organisms, toxicity to non-targeted species, damage to human health and development of resistance towards chemical insecticides. The present study is an attempt to explore potent larvicidal efficacy of biofabricated CuNPs of AmC in comparison to CuNPs (130-200 nm) synthesized by chemical reduction method.

Mosquito culture

Larvae of *Anopheles stephensi, Aedes aegypti* and *Culex quinquefasciatus* were collected from rice field, stagnant water and chemical drains surrounding the area of puliyathangal (12.9282 ºN, 79.3324 ºE), Sipcot area, Ranipet, Vellore district, Tamilnadu, India. The collected larvae were identified by Dr. K. Gopalarathinam, senior entomologist, Dept of Public Health & Preventive Medicine, Zonal Entomologist Team (Z.E.T), Velapadi, Vellore (12.9202 ºN, 79.1333 ºE) district, Tamilnadu, India. To start the colony, all the collected larvae were kept in plastic trays containing tap water. The larvae were fed with wheat flour, brewer's yeast and algae which were collected from ponds in the ratio of 4:2:1. All the experimental conditions were carried out at 28 ± 2 ^{o}C under relative humidity of 85-90%.

Larvicidal activity

Standard protocol of WHO was adopted for this study with slight modification. Various concentrations 250, 500 and 1000 ppm of CuNPs of AmC and AmC crude leaf extracts was prepared from stock solutions. 30 early third instar larvae were introduced into the petridish containing 200 ml of distilled water with each concentration of extract. A total of 4 trials with 5 replicates were carried out per each trail against blood feeding larvae. A control was maintained by adding only distilled water excluding the plant leaf extracts and CuNPs of AmC. After 24 h the percent mortality rate of blood feeding mosquitoes was calculated and compared to that of standard Temephos (Larcon 50 EC). The results obtained were shown in (Table 3) and graphically depicted in (Fig.6A). When the percent mortality rate of the control ranged from 5-25 % then the observed percentage mortality was corrected by using Abbott's formula.

$$\text{Percentage Mortality:} \quad \frac{\text{Percent mortality in treated} - \text{Percent mortality in control}}{100 - \text{Percent mortality in control}}$$

To further explore the bioefficacy of different CuNPs of AmC (50-100 nm and 100-200 nm) towards antiinflammatory and mosquito larvicidal efficacy, it was compared with the CuNPs synthesized by chemical reduction method by using $NaBH_4$ as reducing agent as described by Qing-ming et al[45] (Supplementary file). A rod shaped CuNPs having face centered cubic structure showing an average particle size of 130-200 nm was prepared and the corresponding XRD, SEM, AFM and size distribution of the nanoparticles were depicted in Fig.10.

3.3 Statistical analysis

All the data were analyzed by using one way factorial ANOVA tests followed by t-test on each group. P values were calculated in each case and accordingly interpretations were carried out. Statistical analysis for larvicidal efficacy of both crude leaf extracts and CuNPs of AmC along with ethylacetate and methanol extracts of AmC were done. Results with $P < 0.05$ were considered statistically significant [46]. The LC_{50} values for larvicidal efficacy of CuNPs of AmC were calculated by linear regression analysis of dose response curve according to Probit methods of Finney [47].

Conclusion

In the field of nanotechnology a critical need is development of reliable, green, one-step, ecofriendly processes for the synthesis of nanoparticles. Here, we have reported biofabrication of CuNps from AmC aqueous leaf extract having spherical shape with face centered cubic structure showing an average particle size of 50-100, 100-200 nm. There is a tremendous increase in surface energy during the formation of CuNPs which makes the extract of AmC biocompatible to the receptor site. Further we evaluated and compared *in-vitro* anti-inflammatory and mosquito larvicidal efficacy of biosynthesized CuNPs of various sizes along with CuNPs from chemical reduction method and the crude leaf extracts. CuNPs of AmC showed good anti-inflammatory activity which was comparable to that of standard Aceclofenac and better larvicidal efficacy against *Anopheles stephensi.* The biofabrication method what we developed is consistent and environmental friendly and can be easily scaled up for the bulk production of nanoparticles rapidly without the generation of toxic byproducts. In future, CuNPs of AmC have immense use as excellent anti-inflammatory agents, drug carriers and also for the control of *Anopheles stephensi* which is considered as an important vector in transmitting malaria.

Notes and references

Organic Chemistry Division, School of Advanced Sciences, VIT University, Vellore 632014, Tamilnadu, India. Fax: 91-416 224 3092; Tel: 0416 220 2352; E-mail: dr.subashini.r@gmail.com.

1. T. Klaus-Joerger, R. Joerger, E. Olsson, C. Granqvist, *Trends in Biotechnology*., 2001, **19**, 15-20.
2. S. Parveen, S. Misra, S. K. Sahoo, *Nanomed-Nanotechnol*., 2012, **8**, 147-166.
3. H. Haberland (Springer Ser.in Chem. Phys., 1994, Vol. 52, Springer-Verlag, Berlin. 2.)
4. C. Templeton, W.P . Wuelfing, R.W. Murray, *Acc.Chem.Res*., 2000, **33**, 27-36.
5. G.G. Ferrier, A.R. Berzins, N.M. Davey, *Platinum Metal Rev*., 1985, **29**, 175-179.
6. H.Bar, D.K. Bhui, G.P. Sahoo, P. Sarkar, S. Pyne, A. Misra, *Colloids and Surfaces A: Physicochem.Eng. Aspects*., 2009, **348**, 212-216.
7. J. Kasturi, S. Veerapandian, N. Rajendiran, *Colloids and Surfaces B: Biointerfaces*., 2009, **68**, 55-60.
8. A.K. Mittal, Y. Chisti, U.C. Banerjee, *Biotechnology Advances.*, 2013, **31**, 346-356.
9. S. Mondal, N. Roy, R.A. Laskar, S.K. Ismail, S. Basu, D. Mandal, N.A. Begum, *Colloids and Surfaces B: Biointerfaces*., 2011, **82**, 497-504.
10. K.P. Kumar, W. Paul, C.P. Sharma, *Process Biochemistry*., 2011, **46**, 2007-2013.
11. K.N.Thakkar, S.S. Mhatre, R.Y. Parikh, *Nanomedicine*., 2010, **6**, 257-262.
12. A.E. Nel, L. Madler, D. Velegol, T. Xia, E.M.V. Hoek, *Nature Materials*., 2009, **8**, 543-557.
13. V.T.P. Vinod, P. Saravanan, B. Sreedhar, D. Keerthi Devi, R.B. Sashidhar, *Colloids and Surfaces B: Biointerfaces*., 2011, **83**, 291-198.
14. A.M. Awwad, N.M. Salem, *Nanoscience and Nanotechnology*., 2012, **2**, 125-128.
15. J. Bland, *Int Clin Nutr Review*., 1984, **4**, 130-134.
16. J.R.J. Sorenson, *J Applied Nutrition*., 1980, **32**, 4-25.
17. G. Berthon, *Agents Actions*., 1993, **39**, 210-217.
18. I. Tenuad, I. Sainte-Marie, O. Jumbou, P. Litoux, B. Dreno, *Br J Dermatol*., 1999, **140**, 26-34.
19. D.H. Brown, W.E. Smith, J.W. Teape, A.J. Lewis, *J. Med. Chem*., 1980, **23**: 729-734.
20. M. Araya, F. Pizarro, M. Olivares, M. Arredondo, M. Gonzalez, M. Mendez, *Biol Res*., 2006, 39, 183-187.
21. G. Borkow, J. Gabbay, R.C. Zatcoff, *Med Hypothesis*., 2008, **70**, 610-613.
22. W. Harless, E. Crowell, J. Abraham, *Am J Hemetol*., 2006, **81**, 546-549.
23. J.D. Huff, Y.K. Keung, M. Thakuri, M.W. Beaty, D.D. Hurd, J. Owen, I. Molnar, *Am J Hematol*., 2007, **82**, 625-630.
24. T. Nagano, T. Toyoda, H. Tanabe, *Intern Med*., 2005, **44**, 554-559.
25. L. Pickart, *J Biomater Sci Polym*., 2008, **19**, 969-988.
26. B.K Rana, U.P. Singh, V. Taneja. *J. Ethnopharmacol*., 1997, **57**, 29-34.
27. L. Badam, S.S. Bedekar, K.B Sonawane, S.P Joshi, *J.Commun Dis*., 2002, **34**, 88-99.
28. G.S.S. Krushna, M.A. Kareem, K.L. Devi, *The Internet Journal of Pharmacology*., 2009, **6**, 2.
29. A.N. Kesari, R.K. Gupta, S.K. Singh, S. Diwakar, G. Watal, *J. Ethnopharmacol*., 2006, **107**, 374-379.
30. S.K. Haravey, *Indian J Med Res*., 1968, **56**, 327-331.
31. S, Dhankar, S, Ruhil, M, Balhara, A.K. Chhillar, *J Med Plants Res*., 2011, 5, 1497-1507.
32. S.M. Roopan, A. Bharathi, R. Kumar, V.G. Khanna, A. Prabakaran, *Colloids and Surfaces B: Biointerfaces*., 2012, **92**, 209-212.
33. J.A. Creighton, D.G. Eadon, *J.Chem.Soc*., 1991, **87**, 3881-3891.
34. D.J. Visurraga, C. Daza, Pozoc, A. Beccerra, V.C.Plessing, A. Giarcia, *Int J Nanomedicine*., 2012, **7** : 3597-3612.
35. M.N.K.Chowdary, M.D.H. Beg, M.R. Khan, M.F.Mina, *Materials Letters*., 2013, **98**, 26-19.
36. H.H.A. Dollwet, J.R.J. Sorenson, *Trace Elements in Medicine*., 1985, **2**, 80- 87.
37. J. Aaseth, T.P. Flaten, O. Anderson, *Scand J Gastroenterol*., 2007, **42**, 673-681.
38. G. Borkow, J. Gabbay, *Curr Chem Biol*., 2009, **3**, 272-278.
39. L. Stella, L. loannis, P.C. George, M. Paraskevi, *Mol. Nutr. Food Res*., 2010, **54**, 551-558.
40. O.S. Canapp, J.P. Farase, G.S. Schults, S. Gowda, A.M. Ishak, S.F. Swiam, J. Vangilder, L.L. Ambrose, E.G. Martin, *Veterinary Surgery*., 2003, **32**, 515-523.
41. J.D.Pollard, S.Quan, T.Kang, R.J.Koch, *Archives of facial plastic surgery*., 2005, **7**, 27-31.
42. C. Winkler, F. Ueberall, D. Fuchs, *Clin.Chem*., 2005, **51**, 2252-2256.
43. S. Singh, J. Tabibian, S.K. Venugopal, S. Devaraj, I. Jialal, *Clin.Chem*., 2006, **52**, 1201-1202.
44. R.C. Dhiman, S. Pahwa, G.P. Dhillon, A.P. Dash, *Parasitol Res*, **106**, 763–773
45. L.Qing-ming, Z.De-bi, Y.Yuya, I.Ryoichi, O.Masazumi, Trans. Nonferrous Met. Soc.China ., 2012, **22**, 117-123.
46. R.R. Sokal, J.F. Rohlf, Biometry principles and practice of statistics in biological research, 2nd edn. WH Freeman and company, New York, 1995, 887.
47. D.J. Finney, Probit Analysis, III edn. Cambridge University Press. Cambridge, England, 1971, 25-325.

FIGURE CAPTIONS

Fig.1 Bioactive compounds identified from leaf extract of AmC.

Fig.2. [A] UV-visible spectrum of mixture of AmC aqueous leaf extract and CuNPs of AmC recorded at various temperatures. [B] Colour change from dark green to light yellow during the formation of CuNps of AmC.

Fig.3. [A] FTIR spectrum of aqueous leaf extract of AmC. [B] FTIR spectrum of CuNPs of AmC. [C] XRD pattern of CuNPs of AmC (50-100 nm). [D] XRD pattern of CuNPs of AmC (100-200 nm).

Fig.4. [A] Biosynthesis of CuNPs of AmC (50-100 nm) (magnification at 42000x). [B] Biosynthesis of CuNPs of AmC (50-100 nm) (magnification at 47200x). [C] Size distribution of CuNPs of AmC (50-100 nm). [D] Biosynthesis of CuNPs of AmC (100-200 nm) (magnification at 5000x). [E] Biosynthesis of CuNPs of AmC (100-200 nm) (magnification at 25000x). [F] Size distribution of CuNPs of AmC (100-200 nm). [G] SEM analysis of AmC aqueous leaf extract (Control).

Fig.5. [A] Phytofabrication of CuNPs by AmC aqueous leaf extracts. [B] Plausible reduction mechanism for the formation of CuNPs from AmC aqueous leaf extracts.

Fig.6. [A] AFM image showing the formation of CuNPs (50-100 nm). [B] AFM image showing the formation of CuNPs (100-200 nm).

Fig.7. Synergistic effect of CuNPs and β-sitosterol.

Fig.8. GHK-Cu tripeptide.

Fig.9 [A] Extracellular scavenging efficacy of CuNPs and β-sitosterol. [B] Proposed anti-inflammatory mechanism of action for synthesized CuNPs. **[**C] Larvicidal efficacy of AmC crude leaf extracts and CuNPs of AmC against *Ae.aegpti, An.stephensi and Cx.quinquefasciatus.* [D] Mechanism of action for larvicidal efficacy.

Fig. 10. [A] SEM image of rod shaped CuNPs (130-200 nm) magnification at 25000x. [B] Size distribution of CuNPs. [C] XRD pattern for synthesized rod shaped CuNPs. [D] AFM showing surface morphology of the CuNPs.

List of figures

Fig.1 Bioactive compounds identified from leaf extract of AmC.

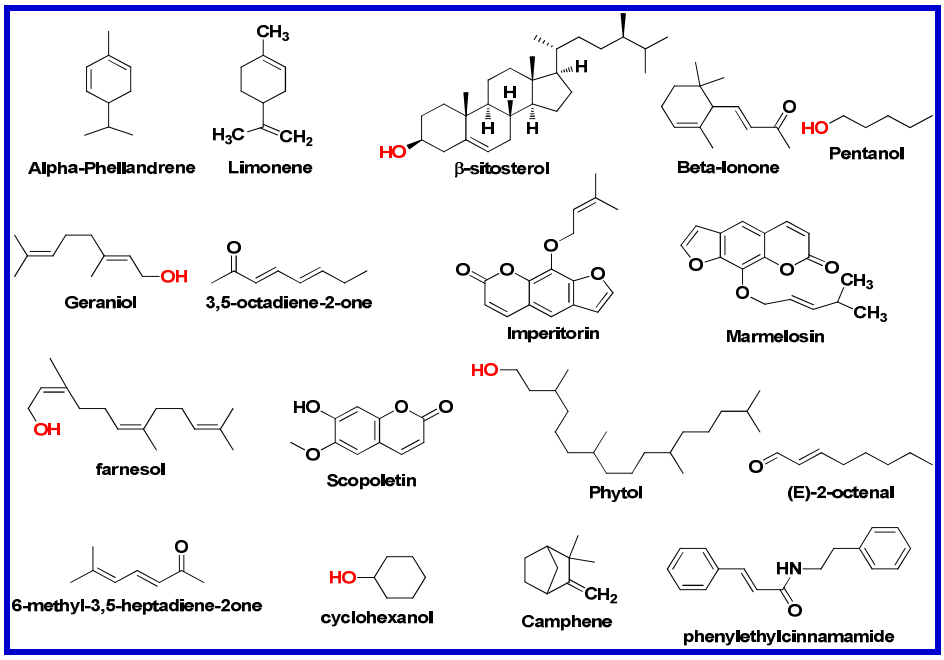

Fig.2. [A] UV-visible spectrum of mixture of AmC aqueous leaf extract and CuNPs of AmC recorded at various temperatures. [B] Colour change from dark green to light yellow during the formation of CuNps of AmC.

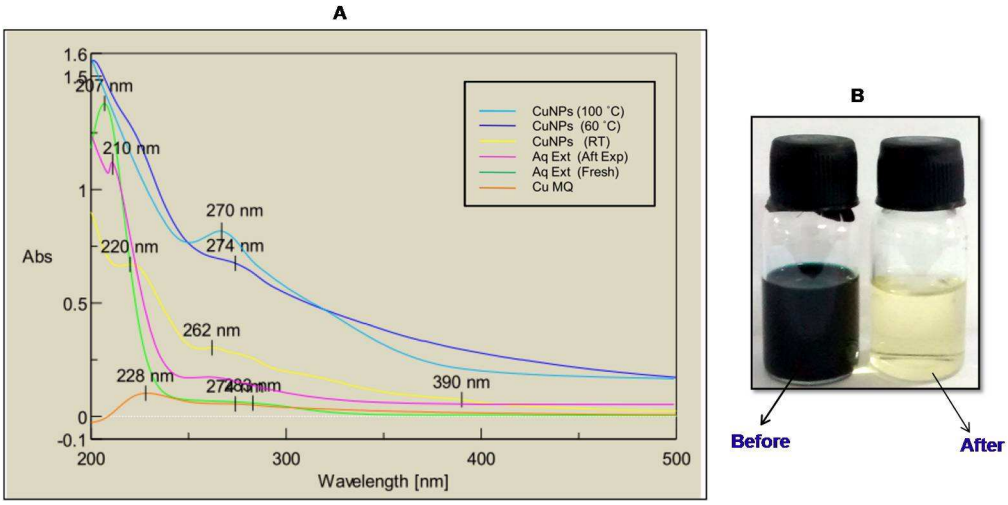

Fig.3. [A] FTIR spectrum of aqueous leaf extract of AmC. [B] FTIR spectrum of CuNPs of AmC. [C] XRD pattern of CuNPs of AmC (50-100 nm). [D] XRD pattern of CuNPs of AmC (100-200 nm).

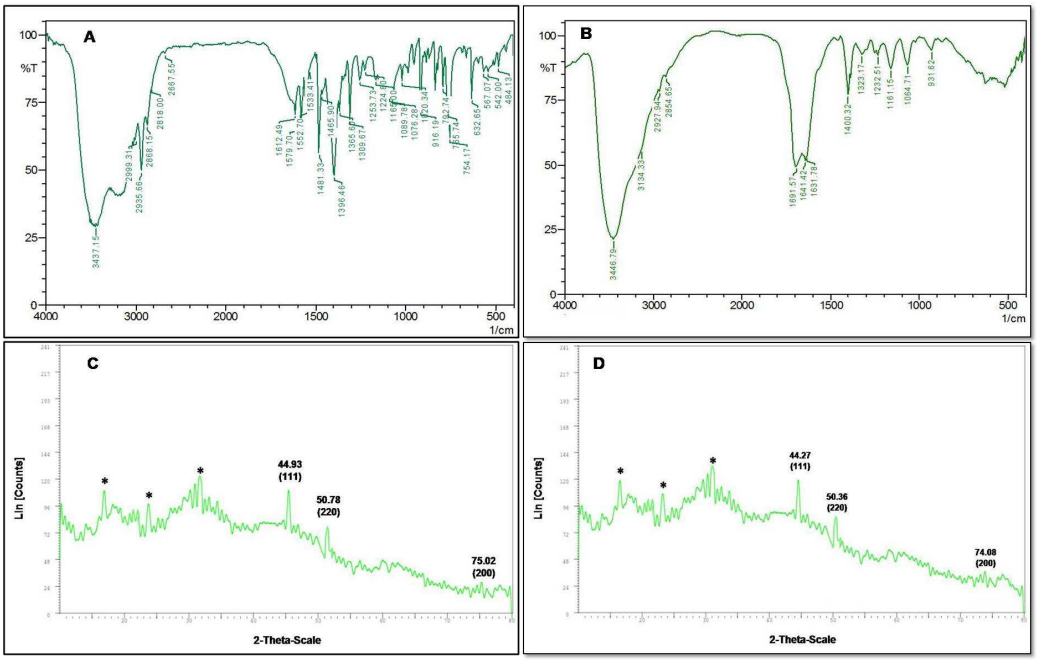

Fig.4. [A] Biosynthesis of CuNPs of AmC (50-100 nm) (magnification at 42000x). [B] Biosynthesis of CuNPs of AmC (50-100 nm) (magnification at 47200x). [C] Size distribution of CuNPs of AmC (50-100 nm). [D] Biosynthesis of CuNPs of AmC (100-200 nm) (magnification at 5000x). [E] Biosynthesis of CuNPs of AmC (100-200 nm) (magnification at 25000x). [F] Size distribution of CuNPs of AmC (100-200 nm). [G] SEM analysis of AmC aqueous leaf extract (Control)

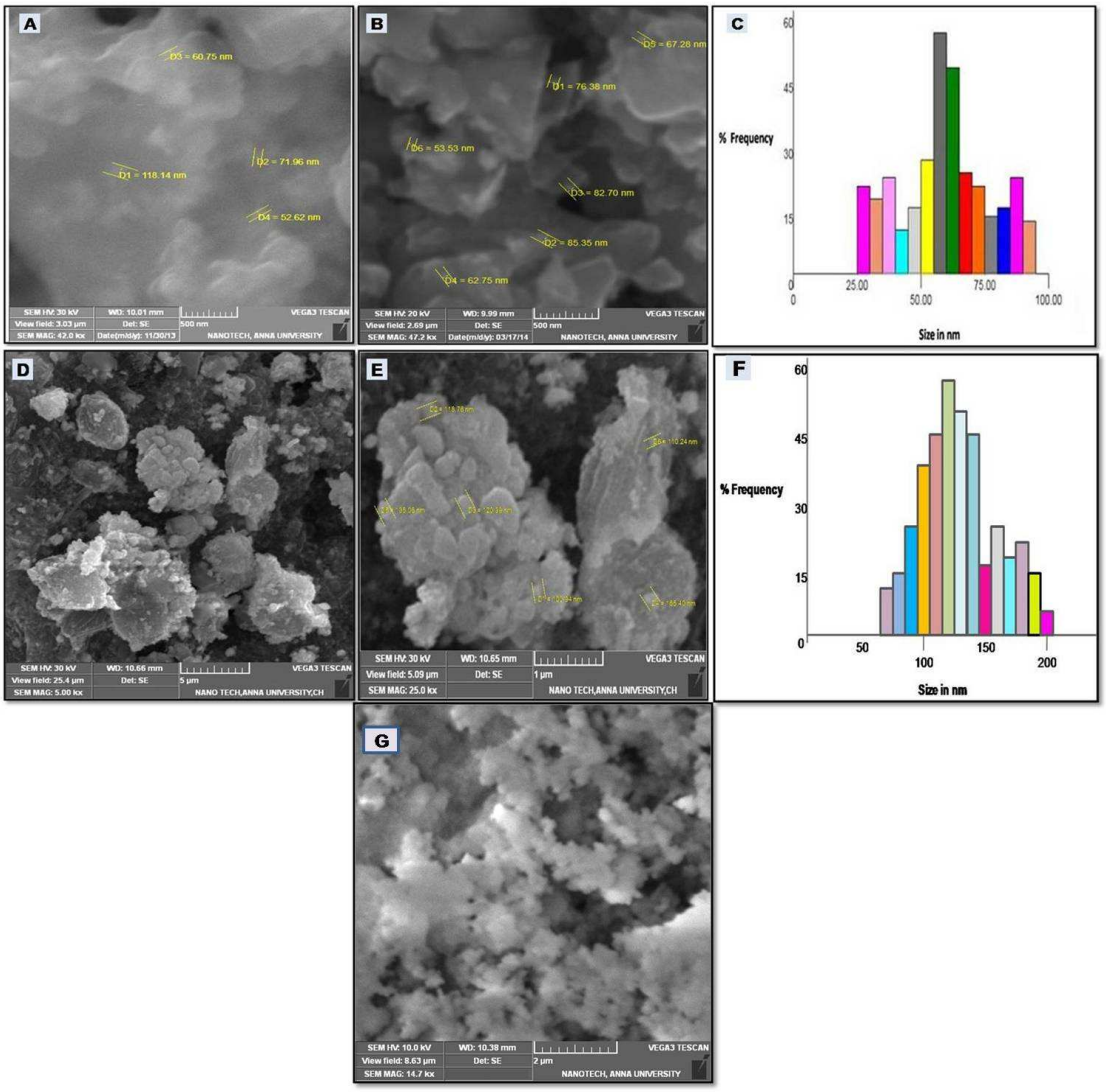

Fig.5. [A] Phytofabrication of CuNPs by AmC aqueous leaf extracts. [B] Plausible reduction mechanism for the formation of CuNPs from AmC aqueous leaf extracts.

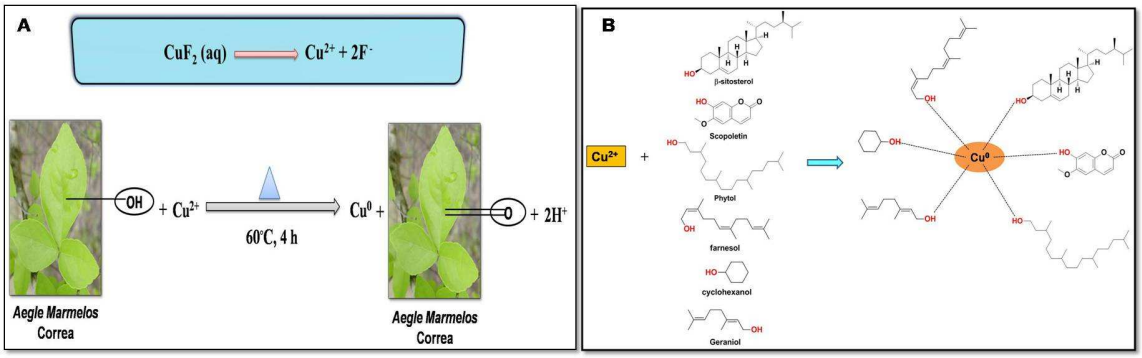

Fig.6. [A] AFM image showing the formation of CuNPs (50-100 nm). [B] AFM image showing the formation of CuNPs (100-200 nm).

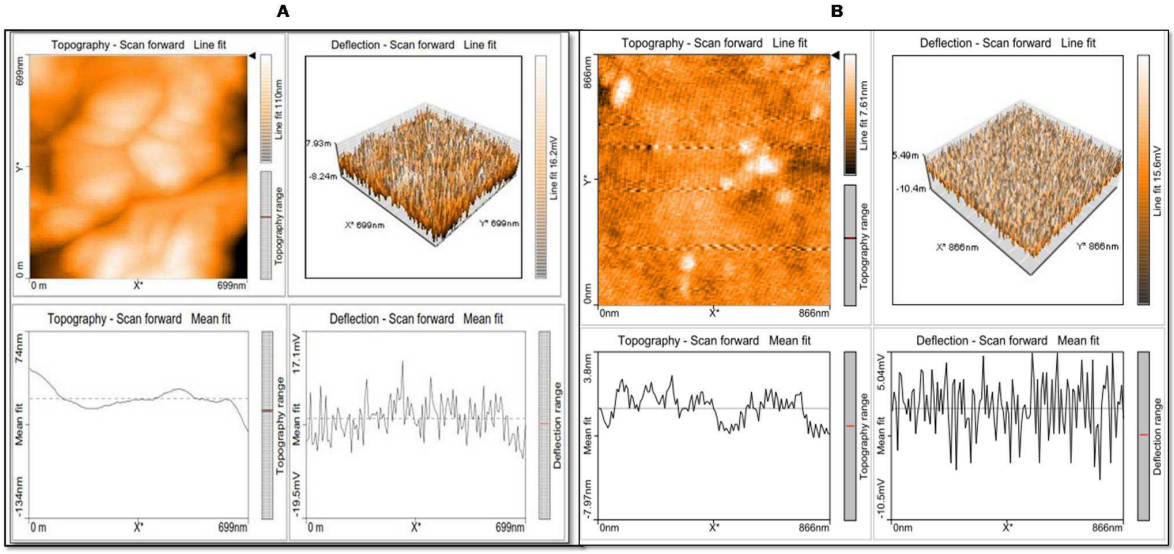

Fig. 7 Synergistic effect of CuNPs and β-sitosterol.

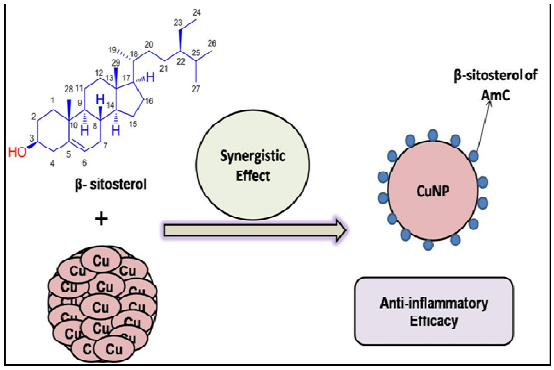

Fig.8. GHK-Cu tripeptide

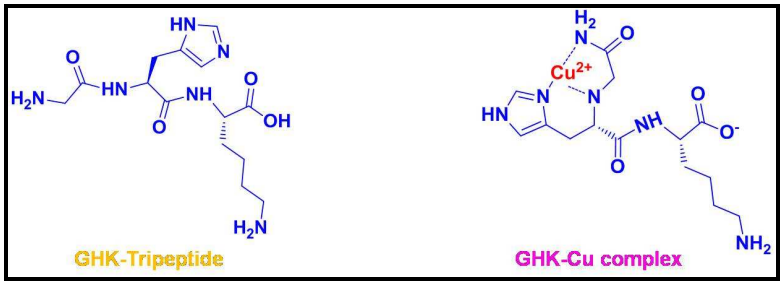

Fig.9 [A] Extracellular scavenging efficacy of CuNPs and β-sitosterol. [B] Proposed anti-inflammatory mechanism of action for synthesized CuNPs. **[**C] Larvicidal efficacy of AmC crude leaf extracts and CuNPs of AmC against *Ae.aegpti, An.stephensi and Cx.quinquefasciatus.* [D] Mechanism of action for larvicidal efficacy.

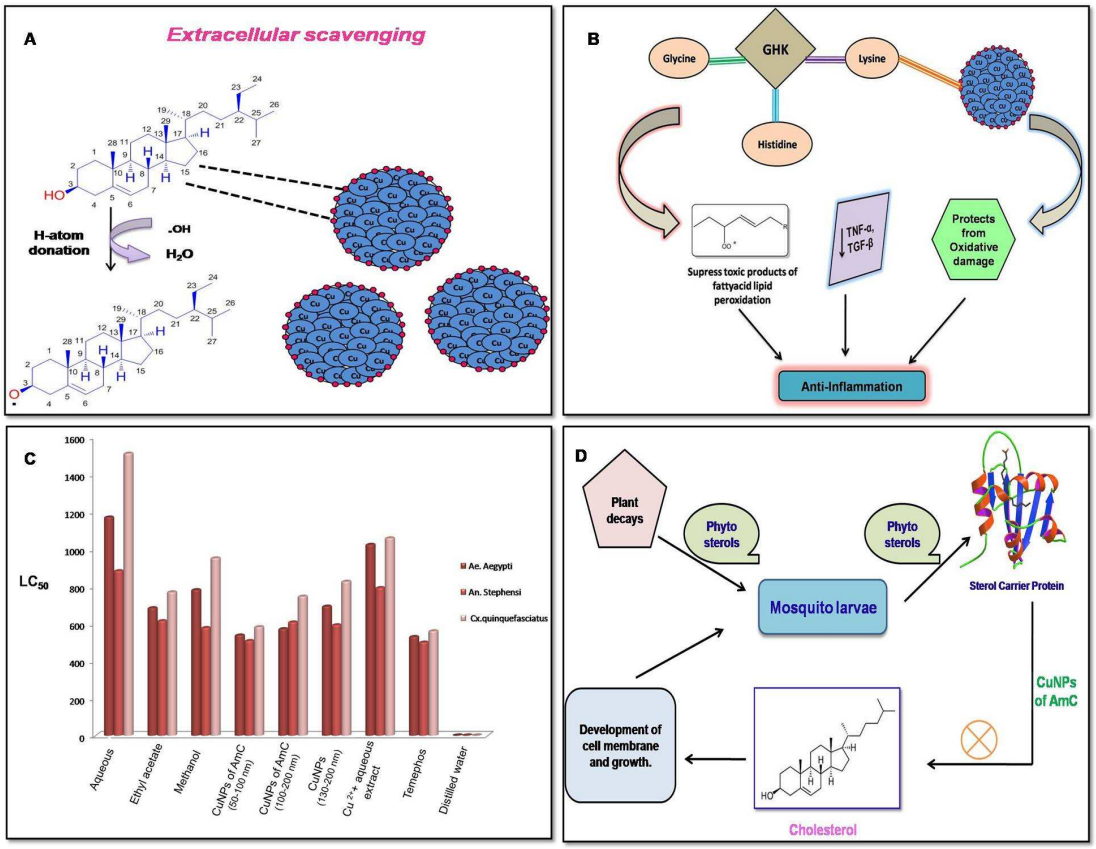

Fig. 10. [A] SEM image of rod shaped CuNPs (130-200 nm) magnification at 25000x. [B] Size distribution of CuNPs. [C] XRD pattern for synthesized rod shaped CuNPs. [D] AFM showing surface morphology of the CuNPs.

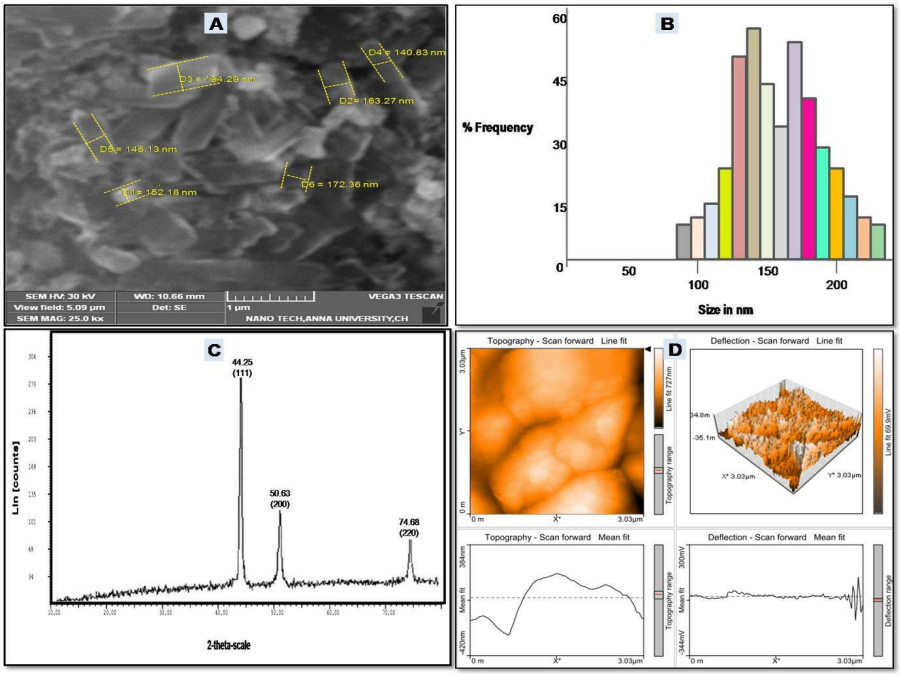

List of tables

Table 1

GC-MS analysis of AmC leaf extract

S.NO	Components	RT	Composition (%)	MW
1	3,5-Octadiene-2-one	17.00	1.02	124.18
2	Cyclohexanol	17.02	2.50	100.15
3	α-Phellandrene	17.07	4.79	136.24
4	β-Ionone	17.27	0.51	192.30
5	Pentanol	17.46	0.62	86.130
6	Geraniol	17.81	0.34	154.24
7	Farnesol	17.81	1.06	222.37
8	6-Methyl-3,5-Heptadiene-2-one	19.65	0.31	124.18
9	Imperitorin	19.85	2.35	270.25
10	Scopoletin	25.55	2.06	192.16
11	Phytol	25.93	2.02	296.00
12	Camphene	27.32	5.67	136.24
13	(E)-2-Octenal	27.44	3.81	126.20
14	Limonene	29.07	3.14	136.24
15	PhenylEthylCinnamide	29.83	4.02	251.13
16	Marmelosin	30.39	3.01	270.27
17	β-Sitosterol	30.98	55.6	414.71
	Total		92.83	

RT-Retention Time; MW: Molecular Weight

Table 2

Membrane stabilizing and Albumin denaturation efficacy of CuNPs and *Aegle marmelos* Correa crude leaf extracts

Membrane stabilizing efficacy				
S.No	Components	Conc (µg/ml)		
		25	50	100
1	Aqueous	24.39 ± 1.47	42.81 ± 0.05	59.40 ± 1.57
2	Methanol	32.21 ± 0.63	63.29 ± 1.75	72.18 ± 0.40
3	Ethyl acetate	28.11 ± 0.14	59.31 ± 0.65	68.14 ± 0.23
4	CuNPs of AmC (50-100 nm)	34.72 ± 1.41	66.75 ± 1.20	78.90 ± 1.23
5	CuNPs of AmC (100-200 nm)	32.04 ± 0.69	62.91 ± 0.25	75.21 ± 0.36
6	CuNPs (130-200 nm)	30.18 ± 1.24	59.20 ± 0.10	70.61 ± 0.47
7	Cu^{2+} + aqueous extract	26.08 ± 0.05	45.13 ± 0.41	62.37 ± 0.38
8	Standard [a]	42.18 ± 1.33	72.81 ± 1.43	88.24 ± 0.86
Albumin denaturation efficacy				
S.No	Components	Conc (µg/ml)		
		25	50	100
1	Aqueous	22.76 ± 0.27	38.40 ± 0.14	55.21 ± 0.22
2	Methanol	28.75 ± 0.87	53.96 ± 1.24	67.13 ± 0.32
3	Ethyl acetate	26.18 ± 0.96	45.62 ± 0.71	61.95 ± 0.59
4	CuNPs of AmC (50-100 nm)	31.94 ± 0.81	58.16 ± 0.16	74.18 ± 1.48
5	CuNPs of AmC (100-200 nm)	29.16 ± 1.05	55.70 ± 0.24	70.26 ± 0.35
6	CuNPs (130 -200 nm)	26.83 ± 0.42	48.26 ± 1.04	65.07 ± 0.62
7	Cu^{2+} + aqueous extract	24.92 ± 1.20	41.07 ± 0.10	60.14 ± 0.26
8	Standard [a]	38.74 ± 0.17	67.32 ± 1.12	84.67 ± 0.19

[a] Aceclofenac

Table 3

Larvicidal efficacy for CuNPs of AmC and AmC crude leaf extracts

Species	Solvents	Mortality rate (%) [Mean ±S.D]			LC_{50} [a] ppm	*df* [b]	t value	P value
		250 ppm	500 ppm	1000 ppm				
Ae. Aegypti	Aqueous	11 ± 1.28	17 ± 1.42	31 ± 1.47	1170.66	5	+2.52	<0.05
	Ethyl acetate	17 ± 1.14	33 ± 1.46	57 ± 0.11	684.44	5	+2.49	<0.05
	Methanol	15 ± 1.71	27 ± 0.57	52 ± 1.12	781.25	5	+2.50	<0.05
	CuNPs of AmC [c]	24 ± 1.64	39 ± 1.05	67 ± 0.04	538.25	5	+2.43	<0.05
	CuNPs of AmC [d]	22 ± 0.31	36 ± 0.14	62 ± 1.05	572.13	5	+2.44	<0.05
	CuNPs [e]	17 ± 1.26	32 ± 0.58	56 ± 0.19	693.05	5	+2.49	<0.05
	Cu^{2+} + aq extract	13 ± 1.84	22 ± 1.47	34 ± 0.50	1024.11	5	+2.51	<0.05
	Positive Control [f]	27 ± 0.47	44 ± 0.53	72 ± 1.72	530.19	5	+2.41	<0.05
	Negative Control [g]	0	0	0	0			
An. Stephensi	Aqueous	13 ± 0.59	23 ± 0.22	39 ± 0.14	882.85	5	+2.52	<0.05
	Ethyl acetate	20 ± 1.88	39 ± 0.44	64 ± 1.02	615.00	5	+2.45	<0.05
	Methanol	21 ± 0.33	41 ± 0.09	62 ± 0.24	578.18	5	+2.44	<0.05
	CuNPs of AmC [c]	27 ± 0.13	43 ± 0.24	69 ± 0.35	508.31	5	+2.42	<0.05
	CuNPs of AmC [d]	24 ± 0.18	41 ± 1.62	65 ± 0.74	608.10	5	+2.44	<0.05
	CuNPs [e]	19 ± 1.05	37 ± 0.24	58 ± 1.03	593.04	5	+2.46	<0.05
	Cu^{2+} + aq extract	15 ± 0.10	28 ± 1.17	52 ± 0.93	792.15	5	+2.51	<0.05
	Positive Control [f]	32 ± 0.34	50 ± 0.46	77 ± 0.49	500.06	5	+2.40	<0.05
	Negative Control [g]	0	0	0	0			
Cx.quinquefasciatus	Aqueous	07 ± 042	13 ± 1.18	25 ± 1.05	1512.50	5	+2.58	<0.05
	Ethyl acetate	17 ± 0.42	27 ± 0.82	53 ± 0.08	769.32	5	+2.51	<0.05
	Methanol	14 ± 1.68	24 ± 1.18	45 ± 0.14	951.53	5	+2.52	<0.05
	CuNPs of AmC [c]	22 ± 1.18	32 ± 1.05	57 ± 1.12	582.73	5	+2.47	<0.05
	CuNPs of AmC [d]	20 ± 0.54	29 ± 0.16	54 ± 0.35	746.08	5	+2.51	<0.05
	CuNPs [e]	16 ± 1.09	25 ± 1.58	49 ± 1.83	826.15	5	+2.52	<0.05
	Cu^{2+} + aq extract	13 ± 0.52	18 ± 1.07	34 ± 0.95	1058.71	5	+2.55	<0.05
	Positive Control [f]	26 ± 0.34	37 ± 0.10	64 ± 0.29	560.82	5	+2.45	<0.05
	Negative Control [g]	0	0	0	0			

[a] Lethal Concentration that kills 50 % of the exposed parasite, [b] degrees of freedom, [c] 50-100 nm, [d] 100-200 nm, [e] chemical synthesis (130 - 200 nm), [f] Temephos, [g] distilled water